THE JOURNAL OF PHYSICAL CHEMISTRY Letters

pubs.acs.org/JPCL Letter

Room-Temperature Electrodeposition of Aluminum via Manipulating Coordination Structure in $AlCl_3$ Solutions

Xiaoyu Wen,[⊥] Yuhang Liu,[⊥] Da Xu, Yifan Zhao, Roger K. Lake,* and Juchen Guo*

Cite This: *J. Phys. Chem. Lett.* 2020, 11, 1589−1593 Read Online

ACCESS | Metrics & More | Article Recommendations | Supporting Information

ABSTRACT: The coordination mechanism of chloroaluminate species in aluminum chloride ($AlCl_3$) solutions in γ-butyrolactone (GBL) is investigated using electrochemical, spectroscopic, and computational methods. The liquid-state ^{27}Al NMR spectroscopy shows a sequence of new species generated in the $AlCl_3$−GBL solutions with increasing $AlCl_3$/GBL ratio. Ab initio molecular dynamics simulation reveals the dynamic coordination process between GBL and $AlCl_3$, and the resultant chloroaluminate species are identified as $[AlCl_2\cdot(GBL)_2]^+$, $AlCl_4^-$, $AlCl_3\cdot GBL$, and $Al_3Cl_{10}^-$. The species are further confirmed by surface enhanced Raman spectroscopy combined with calculated Raman spectra from methods based on density functional theory. Electrochemical deposition of Al is achieved from the $AlCl_3$−GBL solution containing $Al_3Cl_{10}^-$, which is one of the few noneutectic electrolytes for room-temperature Al deposition reported to date.

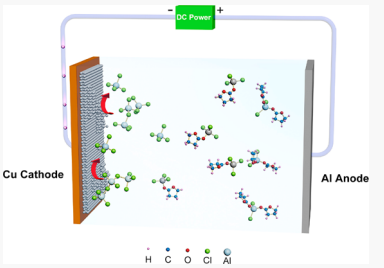

Electrochemical deposition of aluminum (Al) is of significant importance both practically and scientifically. Al deposited on conductive surfaces can be transformed via anodization to a corrosion-resistant aluminum oxide (Al_2O_3) coating, for which there are numerous industrial applications.[1] The emerging technology of rechargeable Al batteries also requires reversible Al deposition as the half-reaction at the anode.[2] However, a lack of feasible electrolytes for Al deposition, particularly at room temperature, has been a steep challenge despite intensive investigation over the past decades. Al cannot be electrodeposited from aqueous solutions due to its very negative reduction potential (−1.67 V vs SHE). Unlike alkali metals (such as lithium and sodium) and alkaline earth metals (such as magnesium), Al has not been successfully deposited from electrolytes of simple Al salts in organic solvents, as even the Al salts have weakly coordinating anions.[3] To date, the majority of electrolytes for Al deposition are eutectic systems including high-temperature molten salts composed of Al halides and alkali metal halides ($AlX_3\cdot MX$, X is Cl^- or Br^- and M^+ is an alkali cation, including Li^+, Na^+, or K^+),[4,5] room-temperature chloroaluminate (bromoaluminate) ionic liquids ($AlX_3\cdot RX$, where X is Cl^- or Br^- and R is an organic cation such as imidazolium, pyridinium, or ammonium),[6,7] and analogues of chloroaluminate ionic liquid including $AlCl_3$/urea[8] and $AlCl_3$/acetamide.[9,10] Despite numerous investigations of electrolytes of $AlCl_3$ in organic solvents, the only successful Al deposition from such electrolytes was from $AlCl_3$ solution in various dialkylsulfones at relatively high concentrations or elevated temperatures.[11,12]

It has been widely recognized that the electrodeposition of Al is attributed to the Lewis acidic $Al_2Cl_7^-$ anion in the $AlCl_3\cdot RCl$ chloroaluminate ionic liquids, which are formed from cleaving Lewis acidic $AlCl_3$ polymer by Lewis basic Cl^-. The Lewis acidity increases, and the anionic species evolves from Reactions 1 to 3 with increasing $AlCl_3/Cl^-$ molar ratio[13]

$$AlCl_3 + Cl^- \rightarrow AlCl_4^- \quad (1)$$

$$AlCl_3 + AlCl_4^- \rightarrow Al_2Cl_7^- \quad (2)$$

$$AlCl_3 + Al_2Cl_7^- \rightarrow Al_3Cl_{10}^- \quad (3)$$

In the other electrolytes that do not contain Cl^-, the formation of $Al_2Cl_7^-$ has not yet been clearly validated and elucidated. An understanding of the formation mechanism of the chloroaluminate species is essential to the development of new Al electrolytes. A common characteristic of dialkylsulfones, urea, and acetamide, which are reported chloride-free components in Al electrolytes, is that they all contain oxygen atoms with lone pair electrons that are considered weak Lewis bases. This characteristic is also shared by many aprotic solvents used in electrochemistry. Therefore, we hypothesize that the formation of chloroaluminate species (and room-temperature Al deposition) is determined by the Lewis acid ($AlCl_3$)−base (solvent) coordination, which is dictated by the species' molar ratio. In this study, we will validate such interactions using the system of $AlCl_3$ in γ-butyrolactone (GBL).

GBL is known as a common solvent in electrochemistry due to its good solubility and stability. $AlCl_3$ solution (1 M) in GBL was actually studied for Al deposition in 1999, but no Al

Received: January 25, 2020
Accepted: February 10, 2020
Published: February 10, 2020

https://dx.doi.org/10.1021/acs.jpclett.0c00256
J. Phys. Chem. Lett. 2020, 11, 1589−1593

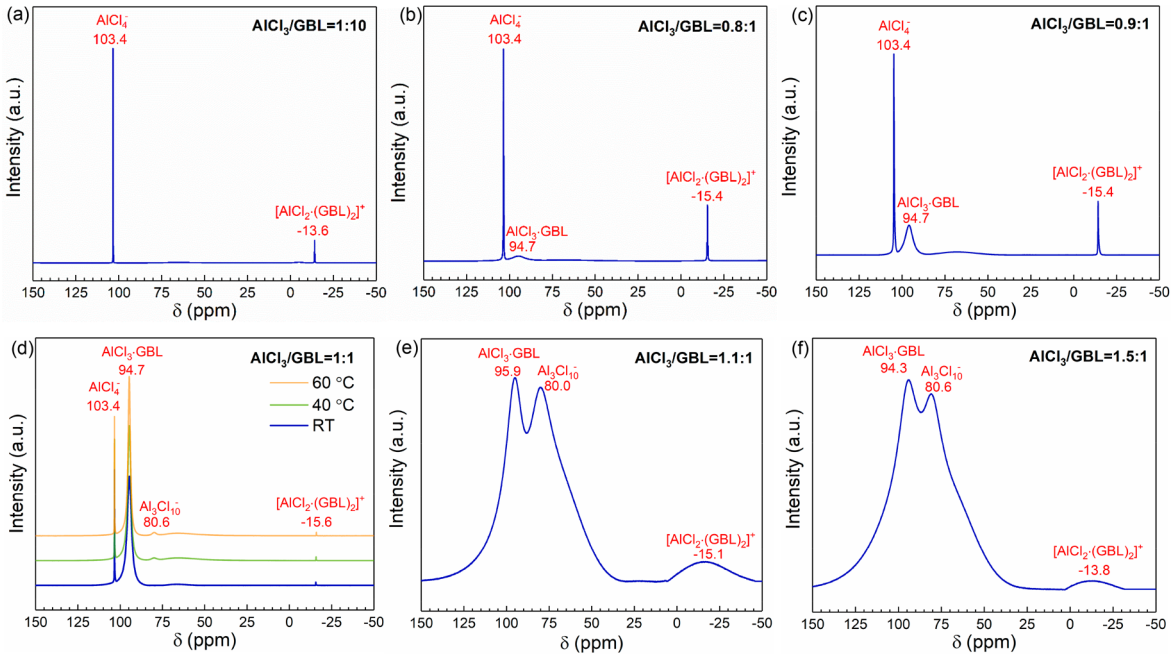

Figure 1. ^{27}Al NMR spectra of $AlCl_3$ solutions in GBL at $AlCl_3$/GBL molar ratios = (a) 1:10, (b) 0.8:1, (c) 0.9:1, (d) 1:1, (e) 1.1:1, and (f) 1.5:1. The ^{27}Al NMR spectra at 1:1 are obtained at room temperature as well as 40 and 60 °C; all the other spectra are obtained at room temperature.

deposition was achieved.[14] The room-temperature ^{27}Al NMR spectrum of 1.3 M $AlCl_3$ in GBL ($AlCl_3$/GBL molar ratio = 1:10) in Figure 1a indicates the existence of two Al-containing species as $AlCl_4^-$ anion (103.4 ppm) and $[AlCl_2\cdot(GBL)_2]^+$ cation (−15.4 ppm), which is consistent with previous findings.[15,16] Both species are known to be inactive toward the electrochemical deposition of Al. The formation of these two species is illustrated by the ab initio molecular dynamics (AIMD) simulation with $AlCl_3$/GBL = 1:10 shown in Scheme 1a. The Al and Cl atoms are labeled for clarity. The detailed calculations are described in the Supporting Information (Figure S1). The dissolution process of $AlCl_3$ can be described as follows: the six-coordinated solid-state $AlCl_3$ is first degraded to the four-coordinated Al_2Cl_6 dimers by coordinating with GBL, forming a transient species Al_2Cl_6·GBL. The Al^2 atom coordinated with GBL in Al_2Cl_6·GBL is further coordinated with a second GBL molecule, thus breaking the Al^2-Cl^6 bond to form an $[AlCl_2\cdot(GBL)_2]^+$ cation and $AlCl_4^-$ anion (Scheme 1a, Reaction 4). This mechanism dominates the chloroaluminate formation at relatively low $AlCl_3$ concentration in GBL. Even when the $AlCl_3$/GBL molar ratio is increased to 1:2.6 (5 M of $AlCl_3$ in GBL), the ^{27}Al NMR spectrum at room temperature is identical to that of the 1:10 ratio (Figure S2), indicating that there is no substantial structural change of the Al species in the solution.

To probe the potential coordination structural change, we further increased the $AlCl_3$/GBL molar ratio. It is worth noting that due to the high viscosity in the high-concentration solutions, benzene, a noncoordinating solvent, was used as the diluent in solutions with an $AlCl_3$/GBL molar ratio higher than 1:2.6. At the $AlCl_3$/GBL molar ratio = 0.8:1, a new peak at 94.7 ppm emerges in the room-temperature ^{27}Al NMR spectrum (Figure 1b), and its relative intensity monotonically increases when the $AlCl_3$/GBL ratio is increased to 0.9:1 and 1:1 (Figure 1c,d). The broad peak at approximately 65 ppm is the background from the Al NMR probe. The 94.7 ppm NMR peak is strong evidence that a new Al-containing species is

Scheme 1. Ab Initio MD Simulations of $AlCl_3$ in GBL at Different $AlCl_3$/GBL Molar Ratios = (a) 1:10, (b) 0.8:1, and (c) 1.5:1

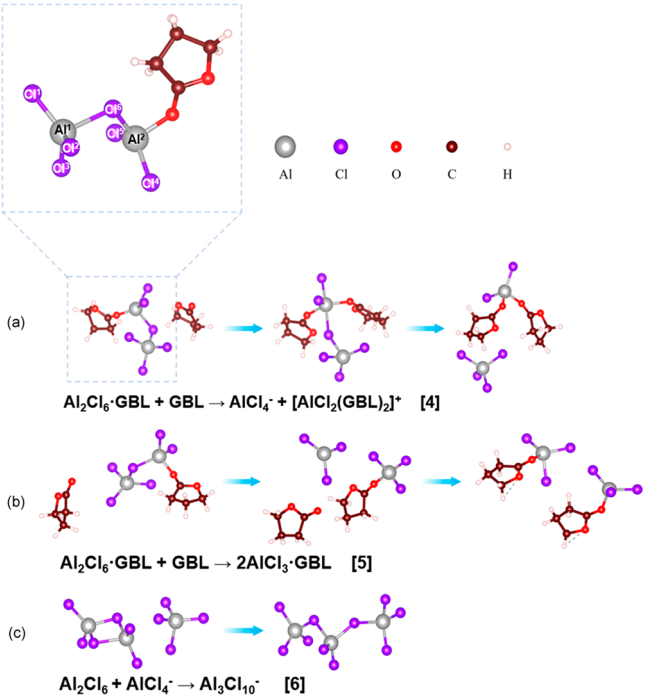

generated. Indeed, the AIMD simulation in Scheme 1b illustrates the formation of a new $AlCl_3$·GBL complex in two steps: When the $AlCl_3$/GBL molar ratio increases, the probability for the second GBL to coordinate with the Al^2 atom (already coordinated with one GBL) in Al_2Cl_6·GBL to break the Al^2-Cl^6 bond is reduced. Instead, the Al^1-Cl^6 bond is able to spontaneously break, due to its lower bond energy than that of Al^2-Cl^6 based on integrated crystal orbital Hamilton populations (Supporting Information). The resulting

https://dx.doi.org/10.1021/acs.jpclett.0c00256
J. Phys. Chem. Lett. 2020, 11, 1589−1593

uncoordinated $AlCl_3$ monomer is subsequently coordinated with a free GBL molecule, thus forming two $AlCl_3$·GBL molecules (Scheme 1b, Reaction 5). The formation of $AlCl_3$·GBL is further supported by the Raman spectroscopy characterization, which will be discussed below.

The room-temperature ^{27}Al NMR spectra at $AlCl_3$/GBL ratios of 1.1:1 and 1.5:1, shown in Figure 1e,f, respectively, show a new peak emerging at approximately 81 ppm, and all peaks becoming broad, indicating the fast dynamic exchange among Al species in the solution. The $AlCl_4^-$ peak at 103.4 ppm either disappears or significantly diminishes under the broad peak of $AlCl_3$·GBL. These two spectra are almost identical to each other but drastically differ from the one with $AlCl_3$/GBL ratio = 1:1. This interesting observation seems to indicate that $AlCl_3$/GBL = 1:1 is a dividing ratio: the solution with $AlCl_3$/GBL = 1:1 is composed of chloroaluminate species including $[AlCl_2\cdot(GBL)_2]^+$, $AlCl_4^-$, and $AlCl_3$·GBL with no free (uncoordinated) GBL molecule. Therefore, we hypothesize that further increasing the content of $AlCl_3$ induces the interaction between the Al_2Cl_6 dimer and $AlCl_4^-$ anion to form the $Al_3Cl_{10}^-$ anion represented by the NMR peak at 81 ppm. The $Al_2Cl_7^-$ anion is not detected, based on the absence of its characteristic NMR peak at approximately 92.7 ppm.[11,17] This mechanism of $Al_3Cl_{10}^-$ formation is confirmed by the AIMD simulation as illustrated in Scheme 1c with Reaction 6 (details in Supporting Information). It is interesting to see that increasing temperature can also induce the formation of $Al_3Cl_{10}^-$ with a lower $AlCl_3$/GBL ratio as clearly indicated by the ^{27}Al NMR spectra of $AlCl_3$/GBL = 1:1 at 40 and 60 °C in Figure 1d. It can be due to the accelerated bond breaking and forming in the solution resulting in the formation of $Al_3Cl_{10}^-$ by the combination of $AlCl_4^-$ anions and Al_2Cl_6 dimers from the transient species Al_2Cl_6·GBL.

In addition to ^{27}Al NMR, surface-enhanced Raman spectroscopy (SERS) was used to analyze the coordination complex in the $AlCl_3$–GBL system as shown in Figure 2. Compared to the SERS spectrum of pure GBL in Figure 2b, the spectrum of solution with $AlCl_3$/GBL = 1:10 shows a new peak at 350 cm^{-1} attributed to the $AlCl_4^-$ anion.[18] It is worth noting that peak(s) representing the $[AlCl_2(GBL)_2]^+$ cation cannot be identified in the spectrum due to possible overlapping with the peaks from GBL. In the SERS spectrum of the solution with $AlCl_3$/GBL = 0.8, the peaks attributed to uncoordinated GBL molecules at 492, 536, 637, 676, and 802 cm^{-1} diminish. The new peak at 608 cm^{-1} is from benzene, which was used as the diluent for the solutions with a high $AlCl_3$/GBL ratio. Two other new peaks at 331 and 425 cm^{-1} clearly emerge in the spectrum, which may be attributed to $AlCl_3$·GBL based on the ^{27}Al NMR result and AIMD simulation. When the $AlCl_3$/GBL ratio is increased to 1:1, the relative intensity of the $AlCl_4^-$ peak at 350 cm^{-1} clearly decreases, with the relative intensity of the peaks at 331 and 425 cm^{-1} increasing. This observation is consistent with our Raman peak assignment. The SERS spectra of solutions with an $AlCl_3$/GBL molar ratio >1 cannot be obtained at the current stage due to the fluorescence effect. To confirm the Raman peaks of $AlCl_3$·GBL, a theoretical Raman spectrum of $AlCl_3$·GBL has been calculated based on density functional theory (DFT) as shown in Figure 2a (computational details in Supporting Information). Based on the calculated Raman spectrum, the peaks at 331, 425, 891, and 937 cm^{-1} are assigned to $AlCl_3$·GBL, and the Raman shift and vibrational modes are summarized in Table 1.

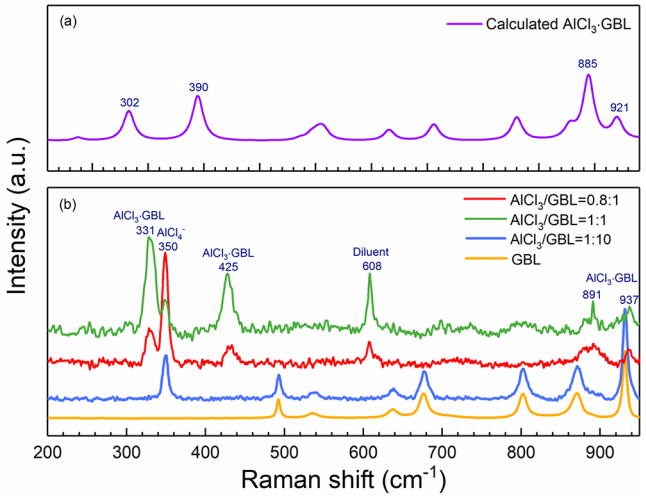

Figure 2. SERS spectra of (a) calculated Raman spectrum of $AlCl_3$·GBL and (b) pure GBL and $AlCl_3$–GBL solutions with $AlCl_3$/GBL molar ratios of 1:10, 0.8:1, and 1:1.

Table 1. Raman Vibrational Modes and the Corresponding Peak Positions of $AlCl_3$·GBL from Experiment and DFT Calculation

vibrational modes	expt. (cm^{-1})	calculated (cm^{-1})
Al–O stretching + C_4O circle rotating	331	302
Al–O stretching	425	390
C_4O circle bending + CH_2 rocking	891	885
C_4O circle bending + CH_2 wagging	937	921

Cyclic voltammetry (CV) was used to investigate the electrochemical properties of the $AlCl_3$–GBL solutions with different $AlCl_3$/GBL molar ratios. As shown in Figure 3a, the electrolyte with $AlCl_3$/GBL = 1.5:1, which contains $Al_3Cl_{10}^-$ anions, demonstrates an intensive reduction peak clearly corresponding to Al deposition. On the other hand, no electrochemical reactivity can be observed from the CV curves of all other electrolytes without $Al_3Cl_{10}^-$ anions. Chronopotentiometry was used for Al deposition on a copper substrate from the electrolyte with $AlCl_3$/GBL = 1.5:1. The X-ray diffraction (XRD) pattern of the deposited layer unambiguously demonstrates metallic Al (Figure 3b). The scanning electron microscopic (SEM) image of the surface morphology of deposited Al is displayed in Figure 3c. The energy dispersive X-ray (EDX) spectrum and elemental mapping in Figure 3d confirm the uniform deposition of Al. The chronopotentiometry experiment in electrolyte with $AlCl_3$/GBL = 1.2:1 also yielded excellent metallic Al deposition (Figures S3a and S4a in the Supporting Information). On the other hand, the same experiment in electrolyte with $AlCl_3$/GBL = 0.8:1 failed to deposit Al (Figures S3b and S4b in the Supporting Information). Based on these results, we propose that the $Al_3Cl_{10}^-$ anion is an electrochemically active species for Al deposition in a similar fashion to $Al_2Cl_7^-$ according to Reaction 7

$$2Al_3Cl_{10}^- + 3e^- \rightarrow Al + 5AlCl_4^- \quad (7)$$

In summary, we demonstrate that Al can be deposited from electrolytes based on $AlCl_3$ in GBL at room temperature by manipulating the coordination structures of $AlCl_3$. ^{27}Al NMR,

https://dx.doi.org/10.1021/acs.jpclett.0c00256
J. Phys. Chem. Lett. 2020, 11, 1589–1593

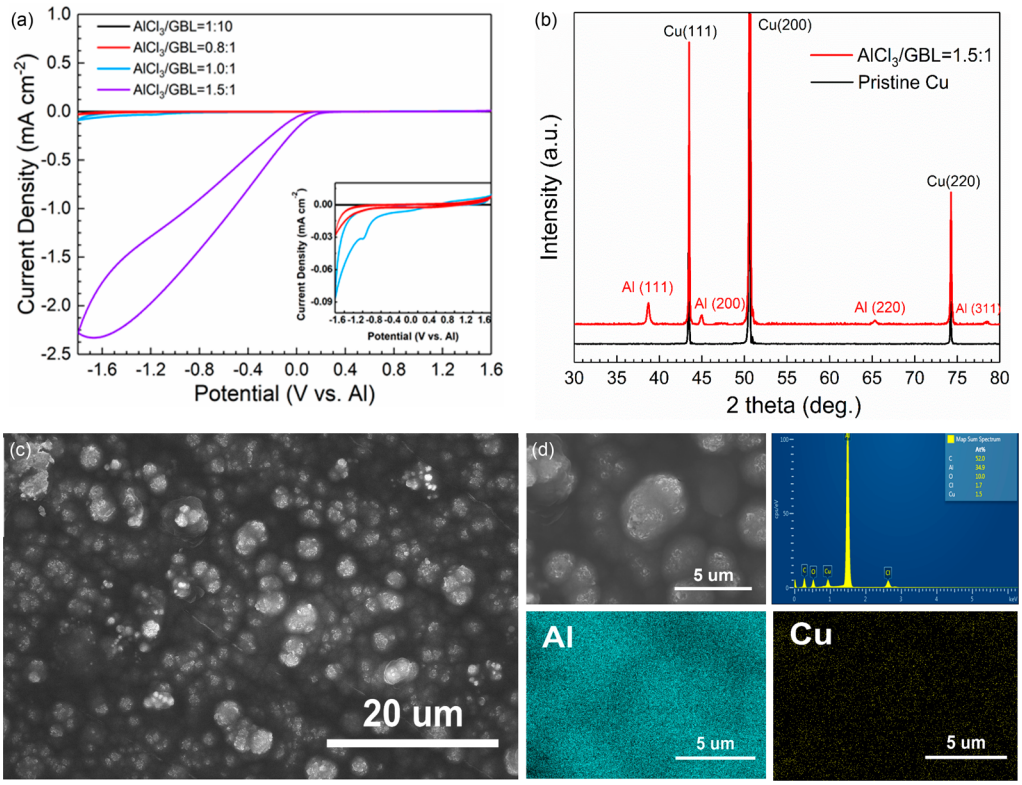

Figure 3. (a) CV scans of electrolyte with $AlCl_3$/GBL = 1:10, 0.8:1, 1:1, and 1.5:1; scan rate is 50 mV s^{-1}. (b) XRD pattern and (c) SEM image of Al deposited on Cu with (d) EDX spectrum from electrolyte with $AlCl_3$/GBL = 1.5:1 at room temperature.

ab initio MD simulation, and SERS collectively reveal the evolution of chloroaluminate species in $AlCl_3$−GBL solutions, which is strongly correlated to the $AlCl_3$/GBL ratio. The electrochemically active $Al_3Cl_{10}^-$ anion is generated from the electrolytes with an $AlCl_3$/GBL ratio >1 at room temperature, from which Al deposition is achieved. Our study provides a new approach to synthesize electrolytes for Al electrodeposition without eutectic systems (ionic liquids). We speculate that similar mechanisms can yield active chloroaluminate species in other systems with $AlCl_3$ and organic solvents containing oxygen atoms with lone pair electrons, which deserve further systematic investigation.

■ ASSOCIATED CONTENT

Supporting Information

The Supporting Information is available free of charge at https://pubs.acs.org/doi/10.1021/acs.jpclett.0c00256.

Experimental and computational methods, ^{27}Al NMR spectrum of $AlCl_3$ in GBL with $AlCl_3$/GBL = 1:2.6, chronopotentiometry curves and SEM characterizations of deposition from electrolytes with $AlCl_3$/GBL at 1.2:1 and 0.8:1, respectively (PDF)

■ AUTHOR INFORMATION

Corresponding Authors

Roger K. Lake − *Department of Electrical and Computer Engineering, University of California, Riverside, California 92521, United States*; Email: rlake@ece.ucr.edu

Juchen Guo − *Department of Chemical and Environmental Engineering and Materials Science and Engineering Program, University of California, Riverside, California 92521, United States*; orcid.org/0000-0001-9829-1202; Email: jguo@engr.ucr.edu

Authors

Xiaoyu Wen − *Department of Chemical and Environmental Engineering, University of California, Riverside, California 92521, United States*

Yuhang Liu − *Department of Electrical and Computer Engineering, University of California, Riverside, California 92521, United States*

Da Xu − *Department of Electrical and Computer Engineering, University of California, Riverside, California 92521, United States*; orcid.org/0000-0002-7554-426X

Yifan Zhao − *Materials Science and Engineering Program, University of California, Riverside, California 92521, United States*

Complete contact information is available at: https://pubs.acs.org/10.1021/acs.jpclett.0c00256

Author Contributions

⊥X.W. and Y.L. contributed equally.

Funding

National Science Foundation: CBET-1751929

Notes

The authors declare no competing financial interest.

■ ACKNOWLEDGMENTS

X.W. and J.G. acknowledge the financial support from the U.S. National Science Foundation (NSF) CAREER program through grant number CBET-1751929. NMR measurements were performed at the Analytical Chemistry Instrumentation Facility at UCR, funded in part by the NSF under grant

number CHE-1626673. This work used the Extreme Science and Engineering Discovery Environment (XSEDE),[19] which is supported by National Science Foundation Grant No. ACI-1548562 and allocation ID TG-DMR130081. Used resources include Stampede2 and Comet.

REFERENCES

(1) Bardi, U.; Caporali, S.; Craig, M.; Giorgetti, A.; Perissi, I.; Nicholls, J. R. Electrodeposition of Aluminium Film on P90 Li−Al Alloy as Protective Coating against Corrosion. *Surf. Coat. Technol.* **2009**, *203* (10−11), 1373−1378.

(2) Geng, L.; Lv, G.; Xing, X.; Guo, J. Reversible Electrochemical Intercalation of Aluminum in Mo_6S_8. *Chem. Mater.* **2015**, *27* (14), 4926−4929.

(3) Mandai, T.; Johansson, P. Haloaluminate-Free Cationic Aluminum Complexes: Structural Characterization and Physicochemical Properties. *J. Phys. Chem. C* **2016**, *120* (38), 21285−21292.

(4) Zhao, Y.; VanderNoot, T. Electrodeposition of Aluminium from Nonaqueous Organic Electrolytic Systems and Room Temperature Molten Salts. *Electrochim. Acta* **1997**, *42* (1), 3−13.

(5) Qingfeng, L.; Hjuler, H.; Berg, R.; Bjerrum, N. Electrochemical Deposition of Aluminum from NaCl-$AlCl_3$ Melts. *J. Electrochem. Soc.* **1990**, *137* (2), 593−598.

(6) Wang, Q.; Zhang, Q.; Lu, X.; Zhang, S. Electrodeposition of Al from Chloroaluminate Ionic Liquids with Different Cations. *Ionics* **2017**, *23* (9), 2449−2455.

(7) Pradhan, D.; Reddy, R. G. Mechanistic Study of Al Electrodeposition from EMIC−$AlCl_3$ and BMIC−$AlCl_3$ Electrolytes at Low Temperature. *Mater. Chem. Phys.* **2014**, *143* (2), 564−569.

(8) Abbott, A. P.; Harris, R. C.; Hsieh, Y.-T.; Ryder, K. S.; Sun, I.-W. Aluminium Electrodeposition under Ambient Conditions. *Phys. Chem. Chem. Phys.* **2014**, *16* (28), 14675−14681.

(9) Li, M.; Gao, B.; Liu, C.; Chen, W.; Shi, Z.; Hu, X.; Wang, Z. Electrodeposition of Aluminum from $AlCl_3$/Acetamide Eutectic Solvent. *Electrochim. Acta* **2015**, *180*, 811−814.

(10) Hu, P.; Zhang, R.; Meng, X.; Liu, H.; Xu, C.; Liu, Z. Structural and Spectroscopic Characterizations of Amide-$AlCl_3$-Based Ionic Liquid Analogues. *Inorg. Chem.* **2016**, *55* (5), 2374−80.

(11) Nakayama, Y.; Senda, Y.; Kawasaki, H.; Koshitani, N.; Hosoi, S.; Kudo, Y.; Morioka, H.; Nagamine, M. Sulfone-based Electrolytes for Aluminium Rechargeable Batteries. *Phys. Chem. Chem. Phys.* **2015**, *17* (8), 5758−66.

(12) Legrand, L.; Heintz, M.; Tranchant, A.; Messina, R. Sulfone-based Electrolytes for Aluminum Electrodeposition. *Electrochim. Acta* **1995**, *40* (11), 1711−1716.

(13) Zhang, M.; Kamavarum, V.; Reddy, R. G. New Electrolytes for Aluminum Production: Ionic Liquids. *JOM* **2003**, *55* (11), 54−57.

(14) Licht, S.; Levitin, G.; Yarnitzky, C.; Tel-Vered, R. The Organic Phase for Aluminum Batteries. *Electrochem. Solid-State Lett.* **1999**, *2* (6), 262−264.

(15) Coleman, F.; Srinivasan, G.; Swadzba-Kwasny, M. Liquid Coordination Complexes Formed by the Heterolytic Cleavage of Metal Halides. *Angew. Chem., Int. Ed.* **2013**, *52* (48), 12582−6.

(16) Atwood, D. A. Cationic Group 13 Complexes. *Coord. Chem. Rev.* **1998**, *176* (1), 407−430.

(17) Wen, X.; Liu, Y.; Jadhav, A.; Zhang, J.; Borchardt, D.; Shi, J.; Wong, B. M.; Sanyal, B.; Messinger, R. J.; Guo, J. Materials Compatibility in Rechargeable Aluminum Batteries: Chemical and Electrochmical Properties between Vanadium Pentoxide and Chloroaluminate Ionic Liquids. *Chem. Mater.* **2019**, *31*, 7238−7247.

(18) Legrand, L.; Tranchant, A.; Messina, R.; Romain, F.; Lautie, A. Raman Study of Aluminum Chloride − Dimethylsulfone Solutions. *Inorg. Chem.* **1996**, *35* (5), 1310−1312.

(19) Towns, J.; Cockerill, T.; Dahan, M.; Foster, I.; Gaither, K.; Grimshaw, A.; Hazlewood, V.; Lathrop, S.; Lifka, D.; Peterson, G. D.; et al. XSEDE: Accelerating Scientific Discovery. *Comput. Sci. Eng.* **2014**, *16* (5), 62−74.

https://dx.doi.org/10.1021/acs.jpclett.0c00256
J. Phys. Chem. Lett. 2020, 11, 1589−1593